

# Displacement memory for flyby

P.-M. Zhang<sup>1\*</sup>, Q.-L. Zhao<sup>1†</sup>, J. Balog<sup>2‡</sup>, P. A. Horvathy<sup>3§</sup>

<sup>1</sup> *School of Physics and Astronomy,*

*Sun Yat-sen University, Zhuhai, China*

<sup>2</sup> *Holographic QFT Group, Institute for Particle and Nuclear Physics,*

*HUN-REN Wigner Research Centre for Physics H-1525 Budapest 114, P.O.B. 49, Hungary*

<sup>3</sup> *Laboratoire de Mathématiques et de Physique Théorique, Université de Tours, (France)*

(Dated: November 15, 2024)

## Abstract

Zel'dovich and Polnarev, in their seminal paper [1] suggested that a gravitational wave generated by flyby would merely displace the particles. We confirm their prediction numerically by fine-tuning the wave profile proposed by Gibbons and Hawking [2], and then analytically for its approximation by a Pöschl-Teller potential. Higher-order derivative profiles proposed for gravitational collapse, etc [2] are shortly discussed.

*Annals of Physics* (accepted)

PACS numbers: 04.20.-q Classical general relativity;

04.30.-w Gravitational waves

---

\* <mailto:zhangpm5@mail.sysu.edu.cn>

† <mailto:zhaoqiang@mail2.sysu.edu.cn>

‡ <mailto:balog.janos@wigner.hu>

§ <mailto:horvathy@univ-tours.fr>

## Contents

<b>I. Introduction</b>	2
<b>II. Flyby: transverse motion</b>	4
<b>III. Pöschl-Teller model for flyby: numerical study</b>	6
<b>IV. Pöschl-Teller model for flyby: (semi-) analytic treatment</b>	9
A. Results	12
B. Asymptotic values	13
C. The $k_m \leftrightarrow m$ relation	14
D. Coefficient of the $\ln(1 - z)$ singularity	14
E. Half-waves	16
1. Pöschl-Teller	16
2. Derived Pöschl-Teller	17
<b>V. Higher-derivative profiles</b>	17
<b>VI. Longitudinal motion</b>	21
<b>VII. Conclusion</b>	22
<b>Acknowledgments</b>	24
<b>References</b>	24

## I. INTRODUCTION

The Displacement Memory Effect (DM) for gravitational waves generated by flyby was proposed by Zel’dovich and Polnarev [1] (see also [2–6]), extending previous work on the Velocity Memory Effect (VM) [7–9]. Our initial investigations [10–12] hinted at, though, that for *randomly chosen* parameters particles initially at rest would fly apart with non-zero velocity, as illustrated, e.g. in FIG. # 12. of ref. [12]. However closer recent scrutiny [13–15] indicates that for certain “magical” values of the wave parameters reminiscent of quantum

numbers we *do get*  $DM$ , highlighted by the vanishing of the velocity outside the Wavezone,

$$\left. \frac{dX}{dU} \right|_{(U = -\infty)} = 0 = \left. \frac{dX}{dU} \right|_{(U = \infty)}. \quad (\text{I.1})$$

This paper extends these results to a more physical realm with particular attention at the analytically solvable Pöschl-Teller -version [13, 15–17]. Then we generalize the flyby result to gravitational collapse and other similar cases by studying models with higher-order derivatives of the (Gaussian or Pöschl-Teller profile) proposed in [2–4].

We start with the 4 dimensional Brinkmann metric [18–20],

$$g_{\mu\nu} dX^\mu dX^\nu = \delta_{ij} dX^i dX^j + 2dU dV + \frac{1}{2} \mathcal{A}(U) \left( (X^1)^2 - (X^2)^2 \right) dU^2, \quad (\text{I.2})$$

where  $\mathbf{X} = (X^i)$  are transverse coordinates and  $U, V$  are light-cone coordinates. Its geodesics are given by,

$$\frac{d^2 X^1}{dU^2} - \frac{1}{2} \mathcal{A} X^1 = 0, \quad (\text{I.3a})$$

$$\frac{d^2 X^2}{dU^2} + \frac{1}{2} \mathcal{A} X^2 = 0, \quad (\text{I.3b})$$

$$\frac{d^2 V}{dU^2} + \frac{1}{4} \frac{d\mathcal{A}}{dU} \left( (X^1)^2 - (X^2)^2 \right) + \mathcal{A} \left( X^1 \frac{dX^1}{dU} - X^2 \frac{dX^2}{dU} \right) = 0. \quad (\text{I.3c})$$

The last equation is solved by solving first eqns (I.3a) - (I.3b) for the transverse trajectory  $\mathbf{X}(U)$  and then lifting it to the gravitational wave spacetime.

Let us recall that geodesic motion posses a conserved quantity referred to as the Jacobi invariant [21–23],

$$\mathbf{m}^2 = -g_{\mu\nu} \dot{X}^\mu \dot{X}^\nu = \text{const}. \quad (\text{I.4})$$

where the dot denotes  $d/dU$ . Discarding tachions, we shall consider  $\mathbf{m}^2 \leq 0$ .

Postponing the study of the  $V$ -motion to Sec.VI, we first focus our attention at the motion in transverse space. FIG.1 suggests that for a random choice of the parameters the outgoing particle has constant nonzero velocity : it exhibits the *velocity effect* (VM). However recent results [13] suggest that for a judicious choice of the amplitude a “miracle” may happen and the outgoing velocity *can* indeed vanish — letting us wonder if this is also true in a broader and more physical context, and for flyby in particular. Our investigations below confirm that this is indeed what happens.

In our previous paper [13] we studied two cases in detail, namely those whose Brinkmann profile  $\mathcal{A}$  is either a simple Gaussian, (III.1), or a Pöschl-Teller potential, (III.2). Both of

them have an integer wave number  $m$ . In Sects. II and III we study what happens for flyby modelled by the *derivative profiles* [2] (II.1) and (III.7), respectively.

## II. FLYBY: TRANSVERSE MOTION

We first study what happens when the profile is the derivative of a Gaussian, proposed by Gibbons and Hawking for flyby in [2],

$$\mathcal{A} \equiv \mathcal{A}^G = \frac{d}{dU} \left( \frac{k}{\sqrt{\pi}} e^{-U^2} \right). \quad (\text{II.1})$$

Its null geodesics are depicted in FIG.1,

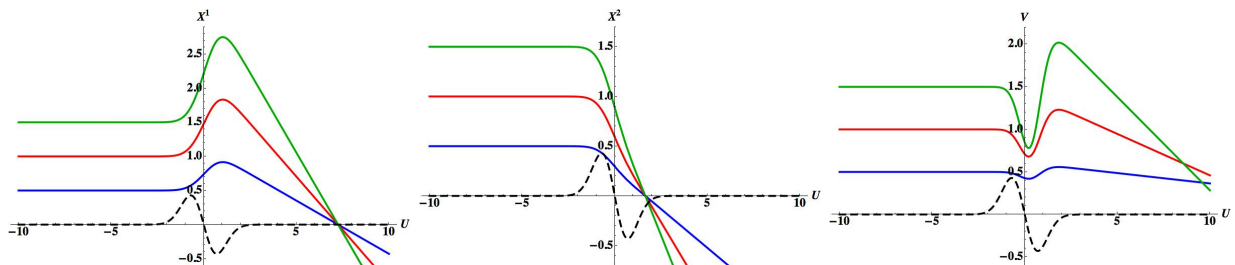


Figure 1: *The null geodesics for the first derivative of the Gaussian in (II.1) shown in the background exhibit, for a randomly chosen fixed amplitude  $k$  but with different initial conditions,  $(0.5, 0.5, 0.5)$ ,  $(1, 1, 1)$ ,  $(1.5, 1.5, 1.5)$ , the velocity effect (VM).*

We start with the massless case,  $\mathbf{m} = 0$ . For randomly chosen amplitude the null geodesics seem to show VM. We study first the transverse motion; that in the  $V$ -direction will be considered in sect. VI. Numerical fine-tuning then indicates that, unexpectedly, for certain “magical” critical values  $k = k_{crit}$  we do get (approximate) DM for both transverse coordinates, as illustrated in FIGs.2 and 3. In fact, we found a well separated discrete series of critical amplitudes,  $k_m$ , each of which corresponding to a unique DM wave labeled by an integer  $m$ ,

$$k_1 = 32.6, \quad k_2 = 97.2, \quad k_3 = 194.8, \quad k_4 = 325.5, \quad k_5 = 489.2 \dots \quad (\text{II.2})$$

Our plots suggest that for each such critical amplitude  $k_{crit}$  the Wavezone contains a unique DM trajectory composed approximately of an integer number of half-waves, consistently with our observations in [13]. The novelty is that DM is now obtained for *both* coordinates.

This is unlike as we had for the simple Gaussian we studied shown in FIG.20 of ref. [13] for which DM could be found, by fine-tuning, in the attractive, but not in the repulsive sector that we call therefore “half-DM”. This behavior is not accidental, as we shall see later.

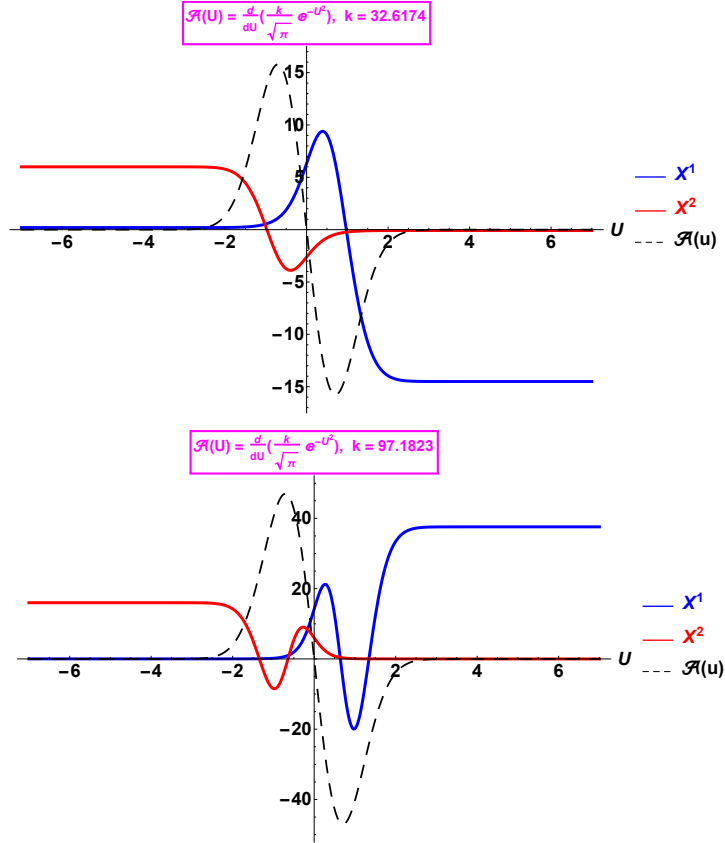


Figure 2: For the flyby profile (II.1) fine-tuning the amplitude yields, for each  $k = k_{crit}$ , a unique (approximate) DM trajectory for both components, as shown for  $\mathbf{m} = 1$  and  $\mathbf{m} = 2$ .

The [square-roots of] the critical amplitude,  $\sqrt{k_{crit}}$ , depend on  $m$  approximately linearly, as shown in FIG.4 (to be compared to FIG.5 of [13]).

For  $k \neq k_{crit}$  we get instead non-zero outgoing velocity; the trajectory is not composed of an integer number of half-waves: we get VM but no DM, as it is manifest in FIG.1.

The behavior for the derivative-Gaussian profile (II.1) for  $m = 1$  and with different initial conditions is shown in FIG.3 for comparison with FIG.1. In the  $U \leq 0$  region the force is repulsive, and in  $U \geq 0$  it is attractive. The strong dependence of the trajectory on the initial position we observe on FIG.3 follows from the “reciprocity constraint” (IV.20), as it will be discussed in section IV.

For generic wave parameters, the particle absorbs some energy from the passing wave

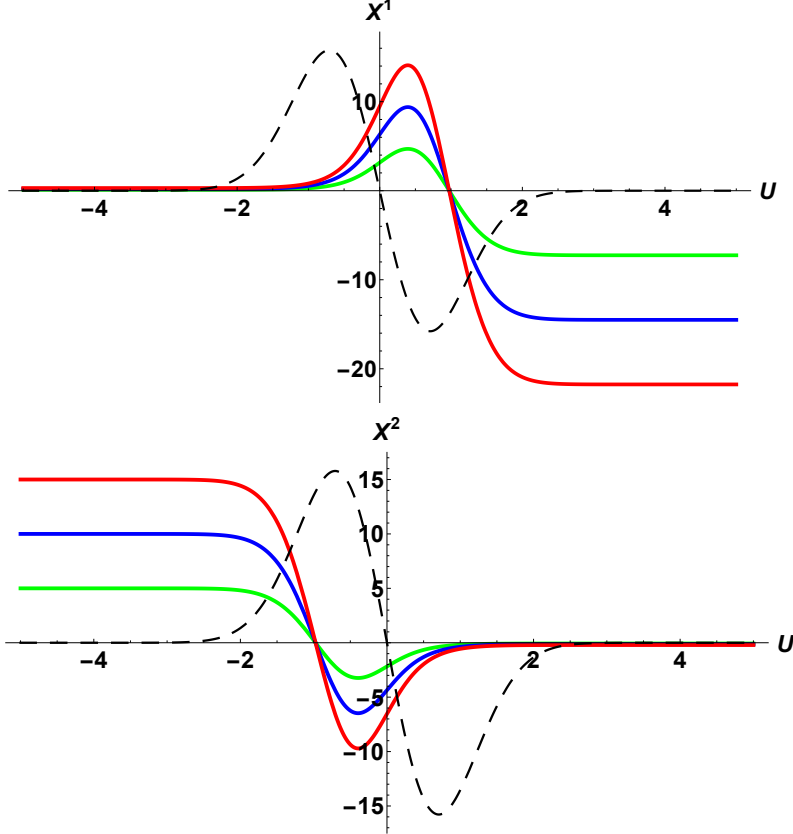


Figure 3: *DM trajectories with (approximate) wave number  $\mathbf{m} = 1$  for the flyby profile (II.1), presented separately for  $X^1$  and for  $X^2$ . The outgoing values depend strongly on the initial conditions, chosen here as  $(0.1, 5)$ ,  $(0.2, 10)$ ,  $(0.3, 15)$ . The parameters were chosen to emphasise the reciprocity relation (IV.20), to be discussed in sec.IV.*

[9, 24, 25]. DM implies in turn zero cumulated energy of the solution in FIG.2, as confirmed in FIG.5. The energy absorption of the underlying NR model [19–21] for  $k_{crit}$  both in the low and high amplitude regimes, is shown in FIG.6. We shall return to the relation with the underlying NR system in sec.VI.

### III. PÖSCHL-TELLER MODEL FOR FLYBY: NUMERICAL STUDY

First we revisit the simplest cases. The geodesics for the Gaussian profile proposed in [2]

$$\mathcal{A}^G(U) = \frac{k}{\sqrt{\pi}} e^{-U^2} \quad (\text{III.1})$$

can only be found numerically. However its similarity with the Pöschl-Teller profile [16],

$$\mathcal{A}^{PT}(U) = \frac{k}{2 \cosh^2 U}, \quad (\text{III.2})$$

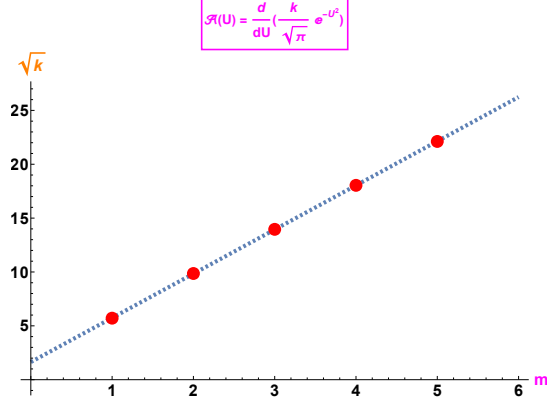


Figure 4:  $DM$  is obtained when the wave number  $m$  and the square-root of the amplitude  $\sqrt{k}$  are (approximately) linearly correlated.

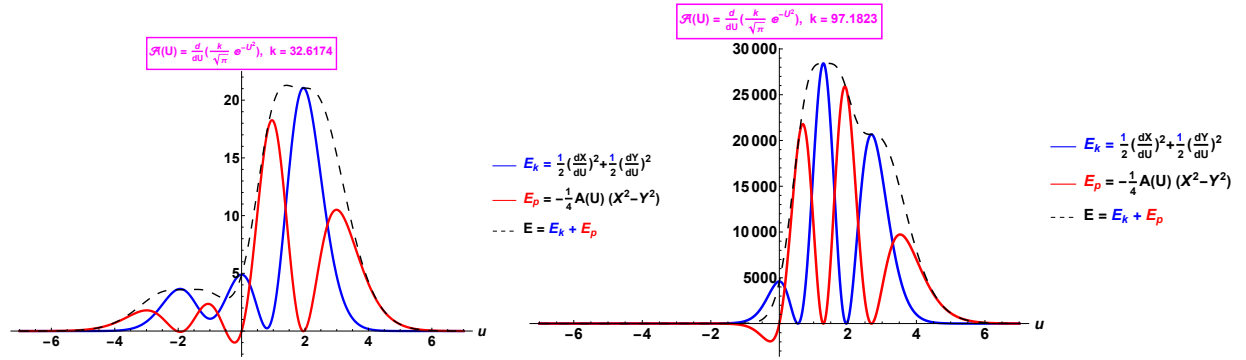


Figure 5: For  $k = k_{crit}$  the total energy balance after the flyby is zero, as shown for  $m = 1$  and for  $m = 2$ .

allowed us to find analytic solutions by solving the Pöschl-Teller-modified Sturm-Liouville equation [13–15, 17]

$$\frac{d^2 X}{dU^2} + \frac{1}{2} \mathcal{A}^{PT} X = 0. \quad (\text{III.3})$$

Putting  $t = \tanh U$  and introducing the (at this point real) parameter  $m$  by

$$k = 4m(m+1) \quad (\text{III.4})$$

(III.3) then becomes the Legendre equation,

$$(1-t^2) \frac{d^2 X}{dt^2} - 2t \frac{dX}{dt} + m(m+1) X = 0. \quad (\text{III.5})$$

Our clue is that the DM conditions (I.1) [or  $X(U = \mp\infty) \rightarrow \text{const.}$ ] require that the solution extends to  $t = \mp 1$ , — yielding a *quantization condition* (see the Conclusion). The

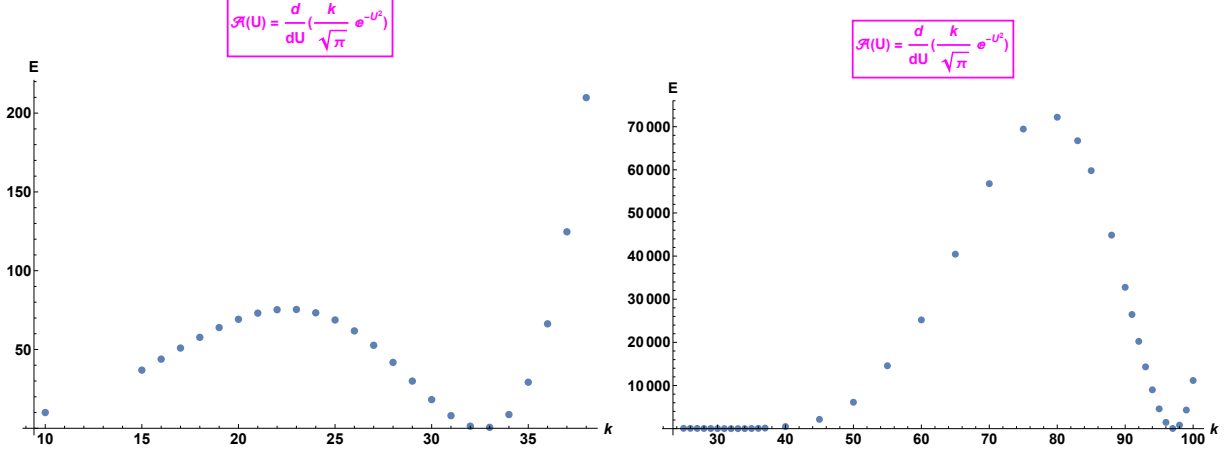


Figure 6: For  $k \neq k_{crit}$  we have VM and the particle extracts some energy from the passing gravitational wave. In the fine-tuned case  $k = k_{crit}$ , though, the cumulative energy balance is zero: the particle does not absorb any energy.

parameter  $m$  must be a natural number,

$$m = 1, 2, \dots \quad (\text{III.6})$$

Then the Legendre *function* which solves eqn. (III.5) truncates to a Legendre *polynomial* of order  $m$ ,  $P_m(\tanh U)$ , see eqn. #(IV.6) and the trajectories exhibit DM, as illustrated in FIGs. # 7, 8, 9 of [13]. In a remarkable analogy with what happens for a harmonic oscillator in Quantum Mechanics [13],  $m \geq 1$  counts *the number of half-waves accommodated in the (approximate) wavezone*. The question will be further discussed in sect.IV.

In  $D = 2$  transverse dimensions the two components come with a relative minus, therefore the two equations in (I.3a)-(I.3b) differ by the sign of  $k$ . Bounded solutions arise only in the attractive sector – Legendre polynomials have  $m \geq 1$  – and we get “half-DM” (as in the Gaussian case [13]).

Turning to *flyby* which is our main concern in this paper, we note that the derivative of the Pöschl-Teller potential (dPT),

$$\mathcal{A} \equiv \mathcal{A}^{dPT} = \frac{d}{dU} \left( \frac{k}{2 \cosh^2 U} \right) = -k \left( \tanh U - \tanh^3 U \right) \quad (\text{III.7})$$

shown in FIG.7 is reminiscent of the derivative-Gaussian proposed in [2], prompting us to study the geodesics of the metric (I.2) with *derivative Pöschl-Teller* (dPT) profile (III.7) as an alternative model for flyby.



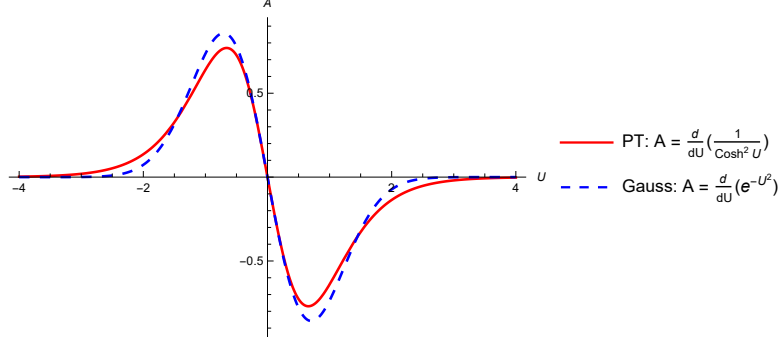


Figure 7: *The derivative of the Pöschl-Teller potential is a good approximation of that of the Gaussian.*

Then we get, instead of (III.5),

$$(1 - t^2) \frac{d^2 X^i}{dt^2} - 2t \frac{dX^i}{dt} \pm \frac{k}{2} t X^i = 0, \quad (\text{III.8})$$

with the  $\pm$  sign referring to the coordinate sector,  $i = 1$  or  $2$ . Assuming  $k > 0$ ,  $+k$  is for  $X^2$  and  $-k$  is for  $X^1$ .

The behavior is reminiscent of but different from that for simple Pöschl-Teller, (III.5), as seen by decomposing (III.8) as,

$$\underbrace{(1 - t^2) \frac{d^2 X^i}{dt^2} - 2t \frac{dX^i}{dt} + 2m(m + 1) X^i}_{\text{Legendre}} - \underbrace{(1 \mp t) 2m(m + 1) X^i}_{\text{perturbation}} = 0. \quad (\text{III.9})$$

where  $m$  is an a priori *real* number. Thus (III.8) is a Legendre eqn. with a linear perturbation. For  $t \rightarrow \pm 1$  both equations become Legendre equations but with different coefficients of the linear term, see FIGs. 8 and 9.

We emphasise, though, that while for the PT profile the analytic calculation is routine-like, the corresponding one for dPT is highly involved, as it will be seen in detail in sect.IV.

We note for completeness that off the critical values,  $k \neq k_m$ , the trajectories exhibit the velocity effect (VM) as expected and illustrated in FIG.10.

#### IV. PÖSCHL-TELLER MODEL FOR FLYBY: (SEMI-) ANALYTIC TREATMENT

Using  $t = \tanh U$  the equations for the transversal components are (III.8),

$$(1 - t^2) \frac{d^2 X^i}{dt^2} - 2t \frac{dX^i}{dt} \pm \frac{k}{2} t X^i = 0,$$

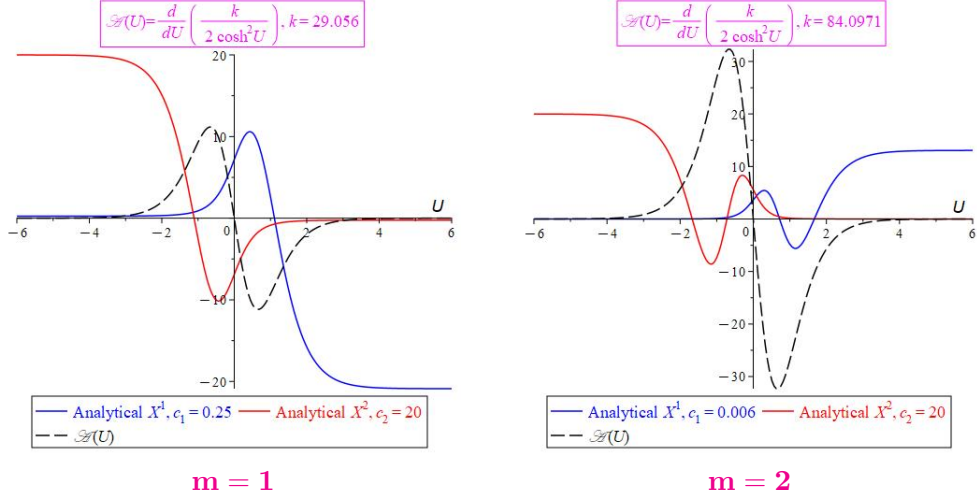


Figure 8: For the dPT-flyby profile (III.7), both numerically or analytically obtained trajectories exhibit DM for both components. For convenience, the  $X^2$  solutions (in red) are rescaled by a factor 20, while the  $X^1$  solutions (in blue) are rescaled, for  $m = 1$ ,  $m = 2$ , by 0.25 and 0.006, respectively.

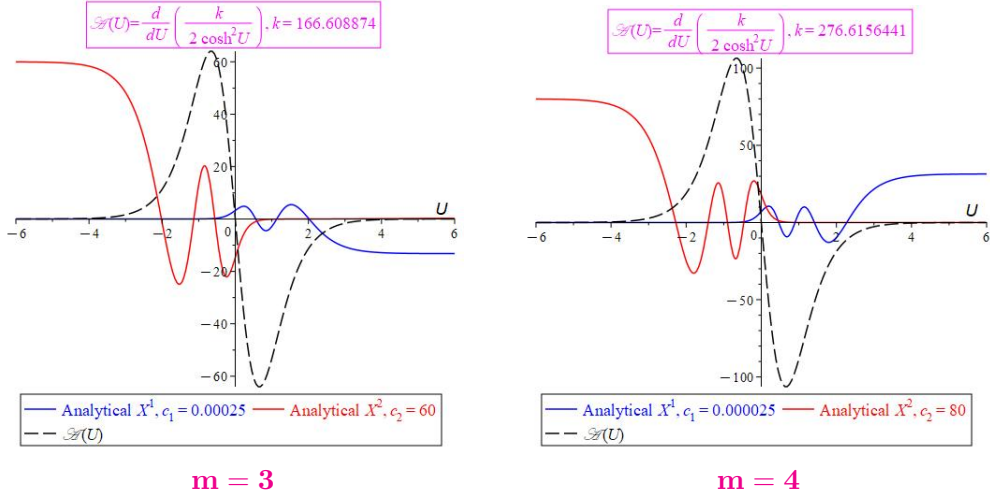


Figure 9: Analytic dPT trajectories for critical amplitude (i)  $k_{crit} = 166. \dots$  and (ii)  $k_{crit} = 276. \dots$  in the derivative-Pöschl-Teller approximation, have half-wave numbers  $m = 3$  and  $m = 4$ .

where the  $\pm$  sign is for the  $i = 1, 2$  components, respectively. We introduce the parameter

$$p = \mp \frac{k}{2} \quad (\text{IV.1})$$

and allows us to study the two cases simultaneously. Changing the independent variable to  $z = \frac{t+1}{2}$  the equation to be solved becomes,

$$\frac{d^2 X}{dz^2} + \left( \frac{1}{z} + \frac{1}{z-1} \right) \frac{dX}{dz} + p \left( \frac{1}{z} + \frac{1}{z-1} \right) X = 0, \quad (\text{IV.2})$$

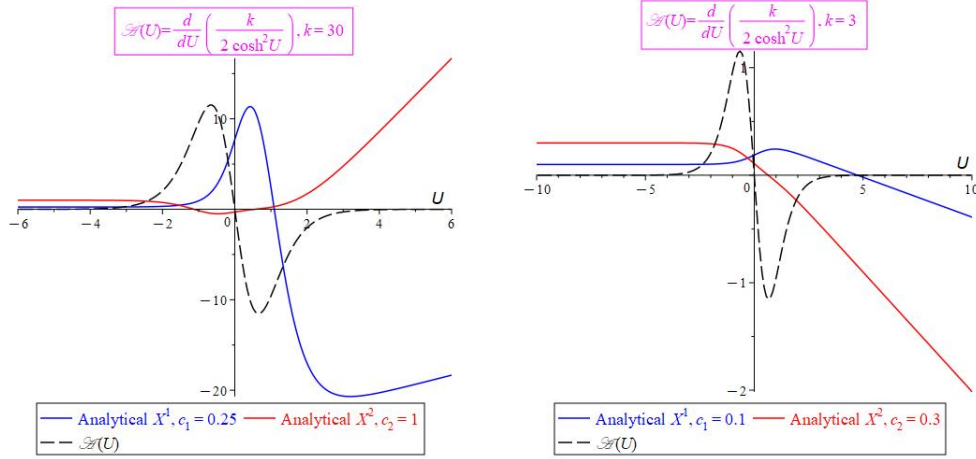


Figure 10: For  $k \neq k_{\text{crit}}$  the trajectories exhibit the velocity effect (VM).

where  $X = X^1$  or  $X^2$ . Here we recognize the *confluent Heun equation* with special parameters. The singular points are  $z = 0, 1$  (plus the irregular singular point at infinity), corresponding to  $t = -1, 1$  and  $U = -\infty, +\infty$ , respectively.

We are looking for solutions which are regular at both of these points. Assuming regularity at  $z = 0$ , we can write the solution as a power series

$$X = \sum_{n=0}^{\infty} s_n z^n. \quad (\text{IV.3})$$

We normalize the solution by putting  $s_0 = 1$ . The  $s_n$  coefficients can be determined from the recursion relation

$$s_{n+1} = \frac{[n(n+1) - p]s_n + 2ps_{n-1}}{(n+1)^2}, \quad n = 0, 1, \dots \quad (\text{IV.4})$$

$s_{-1} = 0$  by convention.

We look for parameter values such that the power series (IV.3), which converges in the disk  $|z| < 1$ , defines a function which is regular also at  $z = 1$ . In similar problems the solution is usually a polynomial. There is no polynomial solution in this case, though.

In the original variable the general solution of the problem behaves as

$$X \sim 2A_0U + \text{const.} \quad (\text{IV.5})$$

for  $U \rightarrow +\infty$ , where  $A_0(p)$  is some parameter-dependent coefficient. In the new coordinates this means singular behaviour,

$$X \sim -A_0 \ln\left(\frac{1-t}{2}\right) = -A_0 \ln(1-z) = A_0 \sum_{n=1}^{\infty} \frac{z^n}{n} \quad (\text{IV.6})$$

for  $t \rightarrow 1, z \rightarrow 1$ . We introduce

$$x_n = ns_n \tag{IV.7}$$

for convenience. According to the above analysis, this has asymptotic expansion for large  $n$

$$x_n = A_0 + \frac{A_1}{n} + \frac{A_2}{n(n-1)} + \frac{A_3}{n(n-1)(n-2)} + \dots \tag{IV.8}$$

with  $p$ -dependent coefficients  $A_k$ . Actually it follows from the recursion relation that all higher coefficients are proportional to  $A_0$ :

$$A_k = \frac{a_k}{k!} A_0, \tag{IV.9}$$

where

$$a_1 = -p, \quad a_2 = p(p-2), \quad p_3 = -p^2(p-8), \quad p_4 = p^3(p-20), \quad \text{etc.} \tag{IV.10}$$

We look for non-singular solutions with  $A_0=0$  for which  $X(U)$  goes to a mere constant when  $U \rightarrow \infty$ , as it follows from (IV.5). According to the above considerations in this case all  $A_k$  vanish and such solutions are not only regular at  $z = 1$  but also analytic there. In fact, these solutions are entire functions.

## A. Results

It remains to find special parameter values  $p_m$  such that

$$A_0(p_m) = 0. \tag{IV.11}$$

(We will also use  $k_m = 2p_m$ .) The trick, which is often used in the case of series behaving asymptotically like (IV.8), is to apply a series of Robertson transformations. These are defined recursively as

$$x_n^{(0)} = x_n, \tag{IV.12}$$

$$x_n^{(s)} = \frac{1}{s} \left\{ (n+1-s)x_n^{(s-1)} - (n+1-2s)x_{n-1}^{(s-1)} \right\}, \quad s = 1, 2, \dots \tag{IV.13}$$

This series of transformations eliminates, step by step, the leading corrections such that for large  $n$

$$x_n^{(s)} = A_0 + O\left(\frac{1}{n^{s+1}}\right), \tag{IV.14}$$

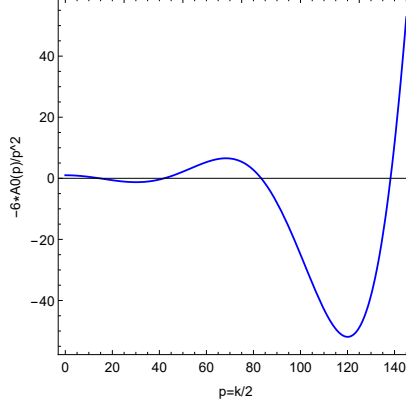


Figure 11: The rescaled  $A_0(p)$  coefficient

i.e. the  $s^{\text{th}}$  Robertson transformed series has the same leading term but much smaller corrections to it. Using this method we calculated (see FIG.11)

$$A_0(p) = -\frac{p^2}{6} \left\{ 1 - \frac{p^2}{180} + 4.036062 \cdot 10^{-6} p^4 - 7.801993 \cdot 10^{-10} p^6 + \dots \right\} \quad (\text{IV.15})$$

The function is even in  $p$  which means that the same critical values work for both signs in the original equation, i.e. the DM condition is satisfied simultaneously for both components  $X^1, X^2$ . The roots of  $A_0(p)$  can only be calculated numerically <sup>1</sup>

$$\begin{aligned} k_1 &= 29.056007, & k_4 &= 276.61564, \\ k_2 &= 84.097092, & k_5 &= 414.12126, \\ k_3 &= 166.608873, & k_6 &= 579.12680. \end{aligned} \quad (\text{IV.16})$$

## B. Asymptotic values

We normalize our solution such that  $X = 1$  at  $U = -\infty$  ( $z = 0$ ). For critical values of  $k$  we can calculate  $X$  at  $U = +\infty$  ( $z = 1$ ). Let us take first  $k = k_1$ . The solution corresponds to the  $X^2$  component and we find

$$X^2(\infty) = -0.01197014 \quad (\text{IV.17})$$

---

<sup>1</sup> The critical values could also be derived readily by requiring that the velocity go to zero when  $U \rightarrow \infty$ , (I.1).

which is very nearly zero. For  $k = -k_1$  instead, which corresponds to the  $X^1$  component, we find the considerably larger value,

$$X^1(\infty) = -83.541230. \quad (\text{IV.18})$$

For  $k = \pm k_2$  the analogous results are

$$X^1(\infty) = 2176.4880, \quad X^2(\infty) = 0.00045945. \quad (\text{IV.19})$$

The necessity to keep so many digits follows from the reciprocity constraint,

$$X^1(\infty)X^2(\infty) = 1, \quad (\text{IV.20})$$

which comes itself from  $U$ -reversal symmetry,

$$U \leftrightarrow -U, \quad (\text{IV.21})$$

which implies in turn  $X^2(\infty) = X^1(-\infty)/X^1(\infty) = 1/X^1(\infty)$  with our normalization.

### C. The $k_m \leftrightarrow m$ relation

The following, purely numerically obtained formulas,

$$k_m = b_0 w_m + b_1 + b_2/w_m, \quad \text{where} \quad w_m = m(m+1), \quad (\text{IV.22})$$

and

$$b_0 = 13.750365, \quad b_1 = 1.61433036, \quad b_2 = -0.11798667 \quad (\text{IV.23})$$

work with rather good precision.

### D. Coefficient of the $\ln(1-z)$ singularity

Summation of the  $A_0$  term gives

$$\sum_{n=1}^{\infty} \frac{z^n}{n} = -\ln(1-z). \quad (\text{IV.24})$$

The higher terms proportional to  $A_1, A_2$ , etc. all contain terms proportional to  $\ln(1-z)$ , but these terms are not singular in the sense that they have finite  $z \rightarrow 1$  limits. Let us parametrize these higher terms as

$$\sum_{n=k}^{\infty} \frac{z^n}{n^2(n-1)(n-2)\dots(n-k+1)} = -c_k \ln(1-z) + r_k. \quad (\text{IV.25})$$

For example,

$$c_1 = -\zeta - \frac{\zeta^2}{2} - \frac{\zeta^3}{3} + \dots \quad r_1 = \frac{\pi^2}{6} - \zeta - \frac{\zeta^2}{4} - \frac{\zeta^3}{9} + \dots \quad (\text{IV.26})$$

$$c_2 = \frac{\zeta^2}{2} + \frac{\zeta^3}{3} + \dots \quad r_2 = 2 - \frac{\pi^2}{6} - \zeta + \frac{\zeta^2}{4} + \frac{\zeta^3}{9} + \dots \quad (\text{IV.27})$$

Here for convenience we introduced the new variable

$$\zeta = 1 - z. \quad (\text{IV.28})$$

The coefficients  $c_k(\zeta)$  start at  $O(\zeta^k)$ , whereas the remainder (analytic) terms  $r_k(\zeta)$  contain all powers of  $\zeta$ . Let us concentrate on the non-analytic term and, using (IV.10), rearrange the power series as

$$\sum_{k=0}^{\infty} A_k c_k(\zeta) = A_0 \sum_{n=0}^{\infty} u_n \zeta^n. \quad (\text{IV.29})$$

For the first few coefficients we find

$$u_0 = 1 \quad u_1 = p \quad u_2 = \frac{p^2}{4} \quad u_3 = -\frac{p^2}{18} + \frac{p^3}{36}. \quad (\text{IV.30})$$

Let us compare this to the first few coefficients of the original power series

$$s_0 = 1 \quad s_1 = -p \quad s_2 = \frac{p^2}{4} \quad s_3 = -\frac{p^2}{18} - \frac{p^3}{36}. \quad (\text{IV.31})$$

We see that they agree up to a sign change. This is not accidental. First of all we see that the differential operator of the confluent Heun equation  $\mathcal{D}X = 0$  is

$$\mathcal{D} = z(z-1) \frac{d^2}{dz^2} + (2z-1) \frac{d}{dz} + p(2z-1), \quad (\text{IV.32})$$

which in the  $\zeta$  variable becomes

$$\mathcal{D} = \zeta(\zeta-1) \frac{d^2}{d\zeta^2} + (2\zeta-1) \frac{d}{d\zeta} - p(2\zeta-1), \quad (\text{IV.33})$$

i.e., it is the same operator with  $p \rightarrow -p$ . Let us write the Ansatz

$$X = -c(\zeta) \ln \zeta + r(\zeta), \quad (\text{IV.34})$$

where we assume that the coefficient functions  $c(\zeta)$  and  $r(\zeta)$  are analytic at  $\zeta = 0$  (power series). Applying the differential operator to this Ansatz we get

$$\mathcal{D}c = 0 \quad \text{and} \quad \mathcal{D}r = 2(\zeta-1) \frac{dc}{d\zeta} + c. \quad (\text{IV.35})$$

From (IV.35) we then see that  $c(\zeta)$  satisfies the  $(-p)$  Heun equation and we find that

$$c(\zeta) = A_0 \text{HeunC}[-p, -2p, 1, 1, 0, \zeta]. \quad (\text{IV.36})$$

This is an alternative way to see that regularity at  $z = 1$  requires  $A_0 = 0$ .

## E. Half-waves

Of course, perfect half-waves are sinusoidal. For  $X(U) = \sin U$  the nodes are at

$$U_1 = 0, \quad U_2 = \pi, \quad U_3 = 2\pi \dots \quad (\text{IV.37})$$

We know that

$$\text{between } U_1 \text{ and } U_2 : \quad X(U) > 0, \quad X''(U) = -\sin U < 0. \quad (\text{IV.38})$$

This means that in this interval the function is *concave* (it bends downwards). In this section we will use *convex* in the sense of the opposite of concave: meaning that the function is bending upwards. Then we see that

$$\text{between } U_2 \text{ and } U_3 : \quad X(U) < 0, \quad X''(U) = -\sin U > 0. \quad (\text{IV.39})$$

In this interval the sine function is convex. Then the whole picture is repeated periodically.

### 1. Pöschl-Teller

In the PT case the function satisfies the differential equation

$$\frac{d^2}{dU^2} X(U) = -\frac{m(m+1)}{\cosh^2 U} X(U) \quad (\text{IV.40})$$

and we have the familiar solution  $X(U) = P_m(\tanh U)$ . Let us denote the roots of the Legendre polynomial (for fixed  $m$ ) by  $y_1, y_2, \dots, y_m$ . Then the nodes of the PT solution are at

$$U_r = \operatorname{arctanh} y_r, \quad r = 1, 2, \dots, m. \quad (\text{IV.41})$$

With our normalization  $X(-\infty) = 1$  and so for  $U < U_1$   $X(U) > 0$  :

$$U_1 < U < U_2 : \quad X(U) < 0, \quad X''(U) > 0. \quad (\text{IV.42})$$

Here the solution is convex, bends back upwards until  $U_2$ . From there on:

$$U_2 < U < U_3 : \quad X(U) > 0, \quad X''(U) < 0. \quad (\text{IV.43})$$

The solution is concave, bends back downwards until  $U_3$ . This alternating pattern repeats itself until  $U_m$ . The solution in each of the intervals is monotonic until the (in this interval



unique) local minimum/maximum is reached; then it is again monotonic towards the next node. This looks like a distorted half-wave.

The main reason of the half-wave-behaviour is that  $X(U)$  and  $X''(U)$  have opposite sign.

Between  $U_1$  and  $U_m$  there are *exactly*  $m - 1$  such distorted half-waves. It is easy to see that this  $m - 1$  counting is correct by plotting

$$m = 1 \quad X(U) = -P_1(\tanh U) = -\tanh U. \quad (\text{IV.44})$$

This solution is monotonic, there is obviously no half-wave as seen in FIG.#7 of [13]. Similarly one can plot

$$m = 2 \quad X(U) = -\frac{1}{2} + \frac{3}{2} \tanh^2 U. \quad (\text{IV.45})$$

There is a single half-wave between  $U_1 = -\text{arctanh}(1/\sqrt{3})$  and  $U_2 = \text{arctanh}(1/\sqrt{3})$ , as seen in FIG.#8 of [13].

Now we turn to flyby, which our main interest in this paper.

## 2. Derived Pöschl-Teller

Here the solution satisfies<sup>2</sup>

$$\frac{d^2}{dU^2} X(U) = -k \tanh U \frac{1}{\cosh^2 U} X(U). \quad (\text{IV.46})$$

As we have seen, for the half-wave-behaviour it is crucial that  $X$  and  $X''$  have opposite sign. In this case this is satisfied only for  $U > 0$ . However, it turns out that this is not a problem. In our normalization  $U(-\infty) = 1$  and so the solution starts off positive. But since initially  $X''$  is also positive, the solution curve is *convex*, so it bends upwards and does not vanish for negative  $U$ . After crossing  $U = 0$  the curve becomes *concave* and now bends downwards until it reaches the first node  $U_1$ . All nodes of  $X^1$  are positive. This means that all our qualitative considerations for the PT case are valid also here: there are exactly  $(m - 1)$  half-waves between  $U_1$  and  $U_m$ .

## V. HIGHER-DERIVATIVE PROFILES

Similar results can be obtained for the higher-derivative profiles proposed in [2, 11, 15].

---

<sup>2</sup> We take here  $X(U) = X^1(U)$ . The considerations for the  $X^2(U)$  coordinate are analogous.

• The system proposed by Braginsky and Thorne [4] corresponds [2] to the *2nd derivative of the Gaussian*,

$$\mathcal{A}^{BT}(U) = \frac{d^2}{dU^2} \left( \frac{k}{\sqrt{\pi}} e^{-U^2} \right). \quad (\text{V.1})$$

A surprising feature which extends our observation made before in the underived case and illustrated in FIG.#(20) of [13] is that DM requires to putting one or the other component to identically zero: and we get *half-DM*, as shown in FIG.12.

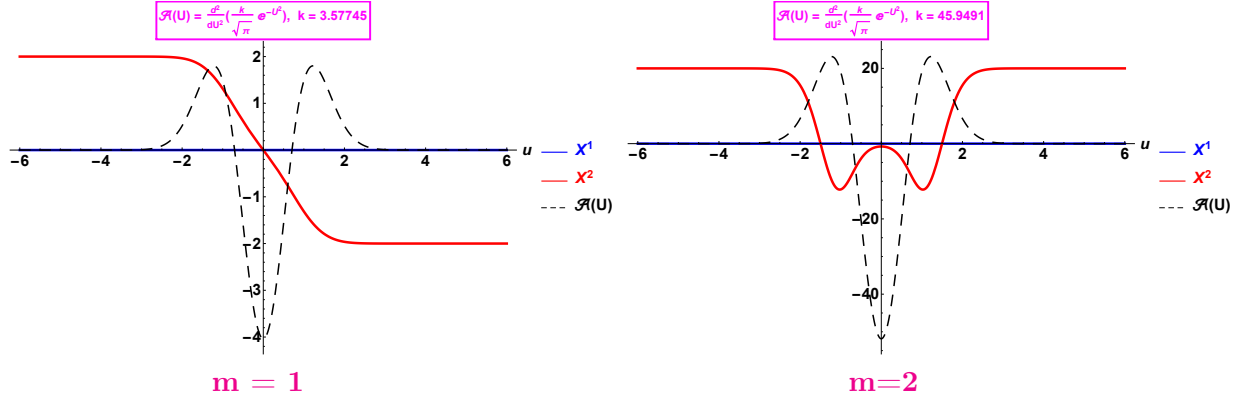


Figure 12: The 2nd-derivative profile (V.1) proposed by Gibbons and Hawking [2] for the Braginsky and Thorne theory [4] has even profile. We can get DM for one (say  $\mathbf{X}^2$ ) coordinate but then the other one should be put to zero,  $\mathbf{X}^1 \equiv 0$ .

This curious “half-sidedness” is explained as follows. Assuming that  $k > 0$ , DM is obtained for  $X^2$  by fine-tuning the amplitude,  $k = k_{crit}^{(2)}$ . This does not work for  $X^1$ , though, unless  $X^1 \equiv 0$ , as confirmed by FIG.13.

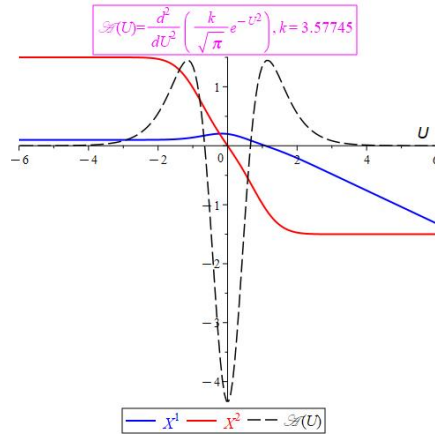


Figure 13: Fine-tuning one of the sectors for DM yields VM for the other component, unless the latter is identically zero.

We could have proceed also with the opposite casting and fine-tune the amplitude for  $X^1$  to get  $k = k_{crit}^{(1)}$ . But the profiles have opposite signs, therefore

$$k_{crit}^{(1)} = -k_{crit}^{(2)}. \quad (\text{V.2})$$

However we have just one  $k$ , and the two choices are consistent only for  $k = 0$ , – i.e., for no wave at all. The only way out is to turn off one of the components, either  $X^1 \equiv 0$ , or  $X^2 \equiv 0$ , depending on the sign of  $k$  : we get *half-DM*. Taking  $k < 0$  the sectors are interchanged.

Not surprisingly, things work along the same lines for the Pöschl-Teller counterpart,

$$\frac{d^2 \mathcal{A}^{PT}}{dU^2} = k \left[ (1 - \tanh^2 U)(1 - 3 \tanh^2 U) \right], \quad (\text{V.3})$$

for which the coefficient of the linear-in- $X$  term in (III.8) is replaced by  $1 - 3t^2$  cf. (III.7), which, for  $t$  close to  $\pm 1$ , multiplies the amplitude by roughly  $(-2)$ . The trajectories shown in FIG.14 are similar to their Gaussian-based counterparts in FIG.12; the only difference is their slightly higher critical amplitude. Numerical evidence suggests that DM trajectories are composed again of (approximately) integer numbers of half-waves.

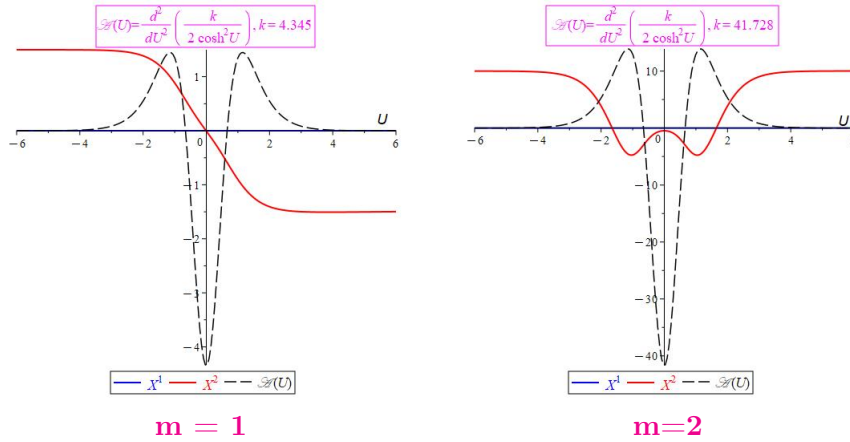


Figure 14: The trajectories for the 2nd derivative of Pöschl-Teller profile are similar to the Gaussian-based versions proposed by Braginsky and Thorne [2, 4], shown in FIG.12.

- The 3rd derivative of the Gaussian

$$\mathcal{A}^{GC}(U) = \frac{d^3}{dU^3} \left( \frac{k}{\sqrt{\pi}} e^{-U^2} \right) \quad (\text{V.4})$$

proposed to describe *gravitational collapse* [2] was studied in some detail in [10, 11] exhibits *DM* again for both components, as shown in FIG.15. The plot of its Pöschl-Teller counterpart is very similar up to having somewhat higher critical parameters,  $k_1 = 4.7457$  and  $k_2 = 31.14958$ , respectively. It is therefore omitted.

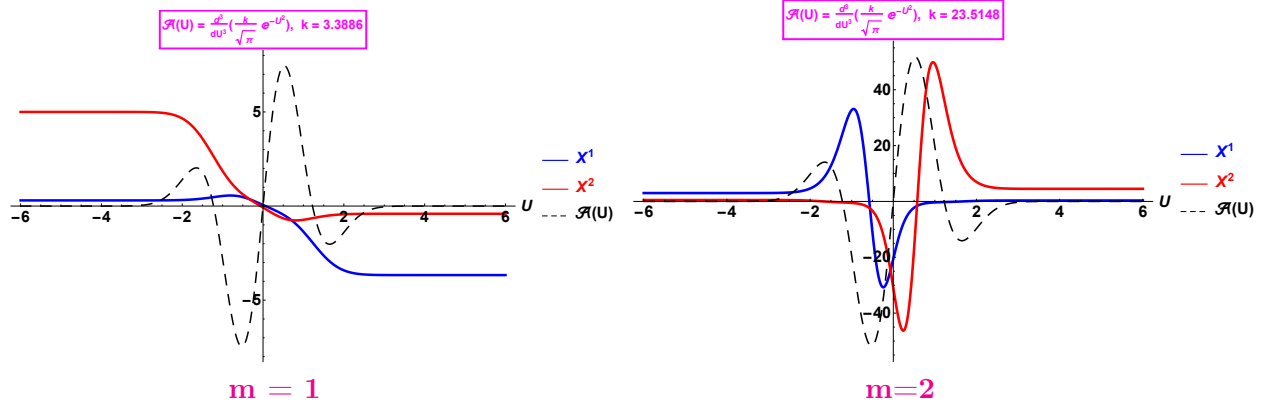


Figure 15: The 3rd derivative of the Gaussian was proposed for gravitational collapse [2]. For  $k_{crit}$  the velocity vanishes at  $U = \pm\infty$ , as required for DM in both components, (I.1).

Models with higher-order derivatives of the Gaussian follow a similar pattern. For the 4th order derivative profile, for example, we would get again half-DM effect, etc.

We now explain the reason by extending our observation related to the behaviour under reversing the sign of  $U$ ,  $U \rightarrow -U$  in (IV.21), We start with an even seed profile,

$$\mathcal{A}^0(-U) = \mathcal{A}^0(U), \quad (\text{V.5})$$

which could be, for example, the Gaussian or Pöschl-Teller as in [13]. Then we consider the profile obtained by deriving  $\mathcal{A}^0$   $\ell$  times,

$$\mathcal{A}^\ell = \frac{d^\ell \mathcal{A}^0}{dU^\ell}. \quad (\text{V.6})$$

The sign-reversal (IV.21) leaves invariant the 2nd-order  $U$ -derivative terms in (I.3) but has an  $\ell$ -dependent effect on the equations of motion :

- for  $\ell = 2n + 1$ ,  $n = 0, 1, \dots$  odd, the profile is *antisymmetric*,

$$\mathcal{A}^{2n+1}(-U) = -\mathcal{A}^{2n+1}(U), \quad (\text{V.7})$$

implying that *the two transverse components in (I.3a)-(I.3b) are merely interchanged* under (IV.21) (as we noticed for flyby in sect.III). Thus they satisfy the same pair of equations

up to permutation. Therefore the DM condition holds either for both or for none of them. When it does, then “*full DM*” is obtained for both coordinates as illustrated in FIGs. 8-9 for  $\ell = 1$ , and in FIG.15 for  $\ell = 3$ .  $U$ -reversal symmetry (IV.21) allows us to generalize our observations in sect.IV.

The parity-dependent behavior is in fact quite general, as it could also be illustrated for example, by the sequence (V.6) with odd seed profile,  $\mathcal{A}^0 \propto \tanh U$  [30].

- for  $\ell = 2n$ ,  $n = 0, 1, \dots$ , *even*, the profile is *symmetric*,

$$\mathcal{A}^{2n}(-U) = \mathcal{A}^{2n}(U). \quad (\text{V.8})$$

Each of the transverse equations (I.3a) and (I.3b) is left invariant under (IV.21)

DM can be obtained by fine-tuning the amplitude in one of the sectors but then the other should be put to zero: we get “*half-DM*”, as illustrated in FIG.# 20 of [13] for  $\ell = 0$  and in FIG.12 for  $\ell = 2$ .

## VI. LONGITUDINAL MOTION

So far we studied motion only in the transverse plane. What about the “vertical” coordinate ? We summarize the answer given in [13]. The projection of motion to transverse space is independent of  $V$  and the parallel-transport eqn. (I.3c) implies, for  $\mathbf{m} = 0$ , that the vertical motion is given by,

$$\hat{V}(U) = V_0 - \int_{-\infty}^U \mathcal{L}_{NR} du, \quad (\text{VI.1})$$

where  $\mathcal{L}_{NR}$  is the underlying non-relativistic Lagrangian, see # (V.1) of [13]. We proved also that the DM conditions  $X'(U = -\infty) = 0 = X'(U = \infty)$  in (I.1) imply that for  $U$  in the Afterzone the integral in (VI.1) vanishes : the classical Hamiltonian action calculated along the underlying NR trajectory should vanish,

$$\int_{-\infty}^U \mathcal{L}_{NR} du = 0, \quad \text{for } U \geq U_a, \quad (\text{VI.2})$$

leaving us with  $\hat{V}(U) = V_0$ . Thus for a massless particle the vertical light-cone coordinate  $V$  does not move at all.

Turning to massive geodesics characterized by the Jacobi invariant  $\mathbf{m} > 0$  in (I.4), the  $V$ -motion is, see # (VI.5) in [13], a mere linear shifted,

$$V(U) = V_0 - \frac{1}{2} \left( \frac{\mathbf{m}}{M} \right)^2 U, \quad (\text{VI.3})$$

where  $M$  is the conserved quantity generated by the Killing vector  $\partial_V$ , interpreted, in the “Bargmann” framework [19, 20], as the underlying NR mass. The massive trajectories are “tilted”, as shown in FIG.#(13) of [13]. However when the relativistic and non-relativistic masses are identical,

$$\mathbf{m} = M. \tag{VI.4}$$

Then setting  $Z = V + \frac{1}{2}U$  we get,

$$Z(U) = V_0 = \text{const.} \tag{VI.5}$$

i.e., we have DM also in the longitudinal  $Z$ -direction, see FIG.#(14) of [13].

## VII. CONCLUSION

Test particles exhibit, generically, the velocity effect (VM) [8, 9, 31] : when hit by a sandwich gravitational wave, the particles fly apart with diverging constant, non-zero velocity [10, 11].

Zel’dovich and Polnarev suggested instead that flyby would approximately generate pure displacement (DM) with vanishing relative velocity [1]. Our main result is to confirm and indeed refine the statement of Zel’dovich and Polnarev. Both numerical and analytical evidence show that a *judicious choice of the wave parameters* yields pure displacement [13].

We emphasise also that the very notion of “wave zone” is problematic. It is, as indicated already by Zeldovich and Polnarev [1], only approximate. How could one define where a Gaussian “ends” ? The answer would depend on the precision. It means, intuitively, “very small”. But if we look at it with a magnifying glass of (say) 100, a trajectory which looked to be constant will become ... oscillating. So the only phrase that we can say rigorously: “the amplitude is smaller than epsilon - and the region where this is so depends on epsilon. We have however a semi-analytical argument: the critical amplitudes listed (IV.16) are the roots of (IV.11) (shown in FIG.11) that we could determine numerically to some accuracy.

Another important clarification about “quantization” : our theory is purely classical, we do *not* consider a quantum theory : we use the word in the sense of Old Quantum Mechanics highlighted by the names of Planck, Bohr, Sommerfeld, etc, who found that certain physical quantities as energy, angular momentum, etc should be “quantized” meaning that they should

take discrete values. Remember that this happened *before* present-day Quantum Mechanics was born.

What is astonishing, though, is that the analogy between classical mechanics/relativity theory and QM goes *beyond* just “taking discrete values”. As noticed in [13], our DM trajectories correspond in fact to solutions of the time-independent Schrödinger equation with growth conditions at infinity. However, no normalizability of the type  $\int |\Psi|^2 < \infty$  is required; on the contrary, we are looking for zero “energy”, non-normalizable solutions, which are not considered in quantum mechanics.

In this paper we study gravitational waves with linearly polarized “plus” profile. Those with “cross” profile are obtained by a rigid rotation and lead to analogous results. Combining the two polarizations is under current investigation.

More generally, we consider gravitational waves whose profile is a derivative of order  $\ell = 0, 1, \dots$  of a seed profile  $\mathcal{A}^0$ , (V.6). The latter can be, for example, a Gaussian [2] or its analytical Doppelgänger, the Pöschl-Teller potential [13, 16, 17]. Other promising candidates (not studied in the paper) could be Rosen-Morse type [37] or inverse-power [15, 38, 39] profiles. Analytically solvable models can be built also from square-profile [15, 32] which have a well-defined wave zone.

This paper extends the above results to a more physical context. We find that DM solutions are composed approximately of an integer number of half-waves which is exact for the simple Pöschl-Teller profile (III.2) and holds approximately for  $\ell = 1$ , as said in [1]. Particular attention is paid to flyby [1], which might approach observability [40–44].

In the generic VM case the particles pick up some energy, which might lead to the absorption of the wave, as discussed quite some time ago. Sect. 2-5.8 of the seminal review of Ehlers and Kundt [9] anticipates much of later work <sup>3</sup>. Although they did not identify either the Carroll symmetry [26–30] or DM, their intuitive argument in their subsec.2-5.8 point in this direction:

*... one finds the effect of a wave pulse on a cloud of resting particles: [their eqn. (2-5.58)] gives the amount of transverse momentum, longitudinal momentum, and kinetic energy [...] a particle has gained [...] after the passage of*

---

<sup>3</sup> We are grateful to P.C. Aichelburg for calling our attention at this.

*the pulse. This consideration suggests convincingly that a cloud of dust is able to extract energy from a gravitational wave [9].*

In this paper we limit our attention at particles at rest before the wave arrives. It is legitimate to wonder, though, what would happen for nonzero initial velocity. In the impulsive case [31, 50, 51] we found merely diverging straight trajectories and no DM, see FIG.#7 of [50].

Preliminary versions of this research were presented by PAH at the Wigner Institute in Budapest (April 5 2024), at the Workshop *Carrollian Physics and Holography\_CDFG\_2024* organised at the Schrödinger Institute in Vienna (April 17 2024) and at the conference “*Conformal anomalies: theory and applications 2024*, <https://indico.math.cnrs.fr/event/10718/> Tours (May 7 2024). P-M Zhang presented related results in [15]. Similar ideas were put forward also in [7, 8, 24, 31]. Recent results on the Memory Effect and the DM or VM puzzle include refs. [32–36].

### Acknowledgments

We are indebted to G. Gibbons for his insights and advices. We benefitted from discussions and correspondence also with P. C. Aichelburg, T. Damour, L. Diósi, M. Elbistan, S. Kar, B. Kocsis, V. Komornik, K. Mitman and S. Silagadze. JB is grateful to SYSU for hospitality extended to him in Zhuhai. PAH thanks the Erwin Schrödinger Institute (ESI, Vienna) for hospitality during the Workshop *Carrollian Physics and Holography\_CDFG\_2024*. The work of JB has been supported in part by the NKFIH grant K134946. PMZ was partially supported by the National Natural Science Foundation of China (Grant No. 12375084).

- 
- [1] Ya. B. Zel’dovich and A. G. Polnarev, “Radiation of gravitational waves by a cluster of superdense stars,” *Astron. Zh.* **51**, 30 (1974) [*Sov. Astron.* **18** 17 (1974)].
  - [2] G. W. Gibbons and S. W. Hawking, “Theory of the detection of short bursts of gravitational radiation,” *Phys. Rev. D* **4** (1971), 2191-2197 doi:10.1103/PhysRevD.4.2191
  - [3] V B Braginsky and L P Grishchuk, “Kinematic resonance and the memory effect in free mass gravitational antennas,” *Zh. Eksp. Teor. Fiz.* **89** 744 (1985) [*Sov. Phys. JETP* **62**, 427 (1985)]



- [4] V B Braginsky and K. S. Thorne, “Gravitational-wave bursts with memory experiments and experimental prospects”, *Nature* **327**, 123 (1987)
- [5] R. K. Sachs, “Gravitational waves in general relativity. 8. Waves in asymptotically flat spacetimes,” *Proc. Roy. Soc. Lond. A* **270** (1962), 103-126 doi:10.1098/rspa.1962.0206
- [6] D. Christodoulou, “Nonlinear nature of gravitation and gravitational wave experiments,” *Phys. Rev. Lett.* **67** (1991), 1486-1489 doi:10.1103/PhysRevLett.67.1486
- [7] L. P. Grishchuk and A. G. Polnarev, “Gravitational wave pulses with ‘velocity coded memory’,” *Sov. Phys. JETP* **69** (1989) 653 [*Zh. Eksp. Teor. Fiz.* **96** (1989) 1153].
- [8] J-M. Souriau, “Ondes et radiations gravitationnelles,” *Colloques Internationaux du CNRS No 220*, pp. 243-256. Paris (1973).
- [9] J. Ehlers and W. Kundt, “Exact solutions of the gravitational field equations,” in *Gravitation: An Introduction to Current Research*, edited by L. Witten (Wiley, New York, London, 1962).
- [10] P.-M. Zhang, C. Duval, G. W. Gibbons and P. A. Horvathy, “The Memory Effect for Plane Gravitational Waves,” *Phys. Lett. B* **772** (2017), 743-746 [arXiv:1704.05997 [gr-qc]].
- [11] P. M. Zhang, C. Duval, G. W. Gibbons and P. A. Horvathy, “Soft gravitons and the memory effect for plane gravitational waves,” *Phys. Rev. D* **96** (2017) no.6, 064013
- [12] M. Elbistan, P. M. Zhang and P. A. Horvathy, “Memory effect & Carroll symmetry, 50 years later,” *Annals Phys.* **459** (2023), 169535 doi:10.1016/j.aop.2023.169535
- [13] P. M. Zhang and P. A. Horvathy, “Displacement within velocity effect in gravitational wave memory,” *Annals of Physics.* **470** (2024) 169784 doi:10.1016/j.aop.2024.169784. [arXiv:2405.12928 [gr-qc]].
- [14] J. Ben Achour and J. P. Uzan, “Displacement versus velocity memory effects from a gravitational plane wave,” *JCAP* **08** (2024), 004 doi:10.1088/1475-7516/2024/08/004 [arXiv:2406.07106 [gr-qc]].
- [15] P. M. Zhang, Q-L Zhao, M. Elbistan and P. A. Horvathy, “Gravitational wave memory effect: further examples,” To appear in : *Proceedings of the 33rd/35th International Colloquium on Group Theoretical Methods in Physics (ICGTMP, Group33/35)*, held in Cotonou, Benin, July 15 - 19, (2024).
- [16] G. Pöschl and E. Teller, “Bemerkungen zur Quantenmechanik des anharmonischen Oszillators,” *Z. Phys.* **83** (1933), 143-151 doi:10.1007/BF01331132
- [17] I. Chakraborty and S. Kar, “Geodesic congruences in exact plane wave spacetimes and the

- memory effect,” *Phys. Rev. D* **101** (2020) no.6, 064022 doi:10.1103/PhysRevD.101.064022 [arXiv:1901.11236 [gr-qc]].
- [18] M. W. Brinkmann, “On Riemann spaces conformal to Euclidean spaces,” *Proc. Natl. Acad. Sci. U.S.* **9** (1923) 1–3; “Einstein spaces which are mapped conformally on each other,” *Math. Ann.* **94** (1925) 119–145.
- [19] C. Duval, G. Burdet, H. P. Kunzle and M. Perrin, “Bargmann Structures and Newton-cartan Theory,” *Phys. Rev. D* **31** (1985), 1841-1853 doi:10.1103/PhysRevD.31.1841
- [20] C. Duval, G.W. Gibbons, P. Horvathy, “Celestial mechanics, conformal structures and gravitational waves,” *Phys. Rev.* **D43** (1991) 3907 [hep-th/0512188].
- [21] L. P. Eisenhart, “Dynamical trajectories and geodesics”, *Ann. of Math.* **30**, 591 (1929).
- [22] M. Elbistan, N. Dimakis, K. Andrzejewski, P. A. Horvathy, P. Kosinski and P. M. Zhang, “Conformal symmetries and integrals of the motion in pp waves with external electromagnetic fields,” *Annals Phys.* **418** (2020), 168180 doi:10.1016/j.aop.2020.168180 [arXiv:2003.07649 [gr-qc]].
- [23] C. Duval, M. Henkel, P. Horvathy, S. Rouhani and P. Zhang, “Schrödinger symmetry: a historical review,” *Int. J. Theor. Phys.* **63** (2024) no.8, 184 doi:10.1007/s10773-024-05673-0 [arXiv:2403.20316 [hep-th]].
- [24] H. Bondi, “Plane Gravitational Waves in General Relativity,” *Nature*, **179** (1957) 1072-1073. doi:10.1038/1791072a0
- [25] D. Kramer, H. Stephani, M. McCallum, E. Herlt, “Exact solutions of Einstein’s field equations,” Cambridge Univ. Press (1980).
- [26] J. M. Lévy-Leblond, “Une nouvelle limite non-relativiste du group de Poincaré,” *Ann. Inst. H Poincaré* **3** (1965) 1;
- [27] N. D. Sen Gupta, “On an Analogue of the Galileo Group,” *Il Nuovo Cimento* **54** (1966) 512.
- [28] H. Bacry and J. Levy-Leblond, “Possible kinematics,” *J. Math. Phys.* **9** (1968), 1605-1614 doi:10.1063/1.1664490
- [29] C. Duval, G. W. Gibbons, P. A. Horvathy and P. M. Zhang, “Carroll versus Newton and Galilei: two dual non-Einsteinian concepts of time,” *Class. Quant. Grav.* **31** (2014) 085016 [arXiv:1402.0657 [gr-qc]].
- [30] C. Duval, G. W. Gibbons, P. A. Horvathy and P. M. Zhang, “Carroll symmetry of plane gravitational waves,” *Class. Quant. Grav.* **34** (2017) no.17, 175003 doi:10.1088/1361-6382/aa7f62

- [arXiv:1702.08284 [gr-qc]].
- [31] P.C.Aichelburg, H.Balasin, “Generalized Symmetries of Impulsive Gravitational Waves,” *Class.Quant.Grav.* **14**:A31-A42, (1997)
- [32] I. Chakraborty and S. Kar, “A simple analytic example of the gravitational wave memory effect,” *Eur. Phys. J. Plus* **137** (2022) no.4, 418 doi:10.1140/epjp/s13360-022-02593-y [arXiv:2202.10661 [gr-qc]].
- [33] K. Mitman, M. Boyle, L. C. Stein, N. Deppe, L. E. Kidder, J. Moxon, H. P. Pfeiffer, M. A. Scheel, S. A. Teukolsky and W. Throwe, *et al.* “A review of gravitational memory and BMS frame fixing in numerical relativity,” *Class. Quant. Grav.* **41** (2024) no.22, 223001 doi:10.1088/1361-6382/ad83c2 [arXiv:2405.08868 [gr-qc]].
- [34] A. I. Harte, T. B. Mieling, M. A. Oancea and F. Steininger, “Gravitational wave memory and its effects on particles and fields,” [arXiv:2407.00174 [gr-qc]].
- [35] A. Hait, S. Mohanty and S. Prakash, “Frequency space derivation of linear and nonlinear memory gravitational wave signals from eccentric binary orbits,” *Phys. Rev. D* **109** (2024) no.8, 084037 doi:10.1103/PhysRevD.109.084037 [arXiv:2211.13120 [gr-qc]].
- [36] A. Dey and S. Kar, “Closed strings in pp-wave spacetimes and the memory effect,” *Phys. Rev. D* **110** (2024) no.8, 084056 doi:10.1103/PhysRevD.110.084056 [arXiv:2407.10095 [gr-qc]].
- [37] D. E. Alvarez-Castillo and M. Kirchbach, “The Real exact solutions to the hyperbolic scarf potential,” *Rev. Mex. Fis. E* **53** (2007), 143-154 [arXiv:quant-ph/0603122 [quant-ph]].
- [38] K. Andrzejewski and S. Prencel, “Niederer’s transformation, time-dependent oscillators and polarized gravitational waves,” doi:10.1088/1361-6382/ab2394 [arXiv:1810.06541 [gr-qc]].
- [39] A. Ilderton, “Screw-symmetric gravitational waves: a double copy of the vortex,” *Phys. Lett. B* **782** (2018) 22 doi:10.1016/j.physletb.2018.04.069 [arXiv:1804.07290 [gr-qc]].
- [40] M. Favata, “Gravitational-wave memory revisited: memory from the merger and recoil of binary black holes,” *J. Phys. Conf. Ser.* **154** (2009), 012043 doi:10.1088/1742-6596/154/1/012043 [arXiv:0811.3451 [astro-ph]].
- [41] M. Favata, “The gravitational-wave memory effect,” *Class. Quant. Grav.* **27** (2010), 084036 doi:10.1088/0264-9381/27/8/084036 [arXiv:1003.3486 [gr-qc]].
- [42] A. Lasenby, “Black holes and gravitational waves,” talks given at the Royal Society Workshop on ‘Black Holes’, Chichley Hall, UK (2017) and KIAA, Beijing (2017).
- [43] P. D. Lasky, E. Thrane, Y. Levin, J. Blackman and Y. Chen, “Detecting gravitational-

- wave memory with LIGO: implications of GW150914,” *Phys. Rev. Lett.* **117** (2016) 061102 [arXiv:1605.01415 [astro-ph.HE]].
- [44] H. Inchauspé, S. Gasparotto, D. Blas, L. Heisenberg, J. Zosso and S. Tiwari, “Measuring gravitational wave memory with LISA,” [arXiv:2406.09228 [gr-qc]].
- [45] P. M. Zhang, C. Duval, G. W. Gibbons and P. A. Horvathy, “Velocity Memory Effect for Polarized Gravitational Waves,” *JCAP* **1805** (2018) no.05, 030 doi:10.1088/1475-7516/2018/05/030 [arXiv:1802.09061 [gr-qc]].
- [46] U. Kol, D. O’connell and O. Telem, “The radial action from probe amplitudes to all orders,” *JHEP* **03**, 141 (2022) doi:10.1007/JHEP03(2022)141 [arXiv:2109.12092 [hep-th]].
- [47] M. Bianchi, D. Bini and G. Di Russo, “Scalar perturbations in a Top-Star spacetime,” [arXiv:2407.10868 [gr-qc]].
- [48] [https://en.wikipedia.org/wiki/Heun\\_function](https://en.wikipedia.org/wiki/Heun_function).
- [49] Plamen P. Fiziev “Novel relations and new properties of confluent Heun’s functions and their derivatives of arbitrary order,” *J. Phys. A: Math. Theor.* **43** (2010) 035203 arXiv:0904.0245 [math-ph] doi 10.1088/1751-8113/43/3/035203
- [50] P. M. Zhang, C. Duval and P. A. Horvathy, “Memory Effect for Impulsive Gravitational Waves,” *Class. Quant. Grav.* **35** (2018) no.6, 065011 doi:10.1088/1361-6382/aaa987 [arXiv:1709.02299 [gr-qc]].
- [51] R. Steinbauer, “The memory effect in impulsive plane waves: comments, corrections, clarifications,” *Class. Quant. Grav.* **36** (2019) no.9, 098001 doi:10.1088/1361-6382/ab127d [arXiv:1811.10940 [gr-qc]].
- [52] Q-L Zhao et al. “Displacement Effect for nonzero initial velocity,” (work in progress)